Published in final edited form as:

Mutat Res Genet Toxicol Environ Mutagen. 2015 April ; 782: 51–56. doi:10.1016/j.mrgentox.2015.03.007.

Analysis of Dibenzo[*def,p*]chrysene-Deoxyadenosine Adducts in Wild-Type and Cytochrome P450 1b1 Knockout Mice using Stable-Isotope Dilution UHPLC-MS/MS

Tod A. Harper Jr.[a,b,c,*], **Jeff Morré**[d,e], **Fredine T. Lauer**[f], **Tammie J. McQuistan**[a,c], **Jessica M. Hummel**[c], **Scott W. Burchiel**[f], and **David E. Williams**[a,b,c,e]

[a]Superfund Research Program, Oregon State University, 1011 ALS, Corvallis, OR, USA 97331

[b]Environmental and Molecular Toxicology Department, Oregon State University, 1007 ALS, Corvallis, OR, USA 97331

[c]Linus Pauling Institute, Oregon State University, 307 LPSC, Corvallis, OR, USA 97331

[d]Department of Chemistry, Oregon State University, 153A Gilbert Hall, Corvallis, OR, USA 97331

[e]Environmental Health Science Center, Oregon State University, 1011 ALS, Corvallis, OR USA 97331

[f]Department of Pharmaceutical Sciences, University of New Mexico, 2502 Marble, NE, Albuquerque, NM 87131

Abstract

The polycyclic aromatic hydrocarbon (PAH), dibenzo[*def,p*]chrysene (DBC; also known as dibenzo[*a,l*]pyrene), is a potent carcinogen in animal models and a class 2A human carcinogen. Recent investigations into DBC-mediated toxicity identified DBC as a potent immunosuppressive agent similar to the well-studied immunotoxicant 7,12-dimethylbenz[*a*]anthracene (DMBA). DBC, like DMBA, is bioactivated by cytochrome P450 (CYP) 1B1 and forms the reactive metabolite DBC-11,12-diol-13,14-epoxide (DBCDE). DBCDE is largely responsible for the genotoxicity associated with DBC exposure. The immunosuppressive properties of several PAHs are also linked to genotoxic mechanisms. Therefore, this study was designed to identify DBCDE-DNA adduct formation in the spleen and thymus of wild-type and cytochrome P450 1b1 (*Cyp1b1*) knockout (KO) mice using a highly sensitive stable-isotope dilution UHPLC-MS/MS method. Stable-isotope dilution UHPLC-MS/MS identified the major DBC adducts (±)-*anti-cis*-DBCDE-dA and (±)-*anti-trans*-DBCDE-dA in the lung, liver, and spleen of both WT and *Cyp1b1* KO mice. However, adduct formation in the thymus was below the level of quantitation for our method. Additionally, adduct formation in *Cyp1b1* KO mice was significantly reduced compared to wild-type (WT) mice receiving DBC via oral gavage. In conclusion, the current study identifies

[*]**Corresponding Author:** Tod Harper Jr., tod.harper@oregonstate.edu, 541-737-6498, 307 LPSC, Corvallis, OR 97331.

for the first time DBCDE-dA adducts in the spleen of mice supporting the link between genotoxicity and immunosuppression, in addition to supporting previous studies identifying Cyp1b1 as the primary CYP involved in DBC bioactivation to DBCDE. The high levels of DBC-DNA adducts identified in the spleen, along with the known high levels of Cyp1b1 expression in this organ, supports further investigation into DBC-mediated immunotoxicity.

Keywords

dibenzo[*def,p*]chrysene; immunosuppression; DNA adduct; Cyp1b1; mass spectrometry; spleen

1. Introduction

Dibenzo[*def,p*]chrysene (DBC; also know as dibenzo[*a,l*]pyrene) is a commonly identified component of polycyclic aromatic hydrocarbon (PAH) mixtures associated with cigarette smoke, coal smoke, and outdoor air pollution [1–3]. The International Agency for Research on Cancer (IARC) classifies DBC as a class 2A probable human carcinogen [4]. In laboratory animals DBC is 30 times more carcinogenic than the well studied benzo[*a*]pyrene (BaP) [4]. Previous reports have shown wild-type (WT) mice orally gavaged with DBC develop cancerous lesions in several tissues including ovaries, lymphoid tissue, and skin [5, 6]. The schematic in Figure 1 represents DBC bioactivation by cytochrome P450 (CYP[1]) 1B1 and epoxide hydrolase (EPHX1) to form the ultimate carcinogen DBCDE [7, 8]. CYP1B1 is primarily responsible for DBC bioactivation evidenced by several *in vitro* studies [9, 10]. Using a *Cyp1b1* knockout (KO) mouse model Buters et al. [5] reported oral exposure to DBC in mice lacking Cyp1b1 resulted in lower tumor formation and restriction of carcinogenic lesions primarily to the lung. Additionally, DBC preferentially forms stable (−)-*anti-cis*-DBCDE-dA and (−)-*anti-trans*-DBCDE-dA adducts at the N^6 position of deoxyadenosine (N^6dA) rather than the N^2 position on deoxyguanine (N^2dG) as with BaP due to the presence of a sterically hindered fjord region [11]. The preferential formation of N^6dA adducts contributes to DBC carcinogenicity as these DNA lesions are more resistant to nucleotide excision repair than N^2dG adducts [12].

PAH genotoxicity is not only associated with carcinogenesis, but also correlated with the immunosuppressive properties of PAHs [13, 14]. Recently, DBC was reported to be strongly immunosuppressive as measured by the T-cell dependent antibody response (TDAR) *ex vivo* model at levels comparable to the proven immunotoxicant, 7,12,-dimethylbenz[*a*]anthracene (DMBA) [15, 16]. Considering the established immunosuppressive properties of DBC this study was designed to examine adduct formation in the spleen and thymus of WT and *Cyp1b1* KO mice using a highly sensitive stable-isotope dilution UHPLC-MS/MS method.

[1]CYP1B1 denotes human protein; Cyp1b1 denotes mouse protein; *CYP1B1* and *Cyp1b1* denotes human and mouse gene, respectively

2. Materials and Methods

2.1 Animals

All animal work was performed with approval from the Institutional Animal and Care Use Committee at Oregon State University. Eight to ten week old male WT (n = 4) (Jackson Laboratories, Bar Harbor, ME) and *Cyp1b1* KO (n = 5) (Dr. Frank Gonzalez, NCI) mice on the same C57BL/6J genetic background were maintained on a 12-hour light/dark cycle with rodent chow and water *ad libitum*. Mice were dosed with 10 mg/kg DBC via oral gavage for 5 consecutive days. The mice were euthanized via CO_2 asphyxiation 3 days after the final exposure. Target tissues (spleen, thymus, lung, liver) were collected, snap-frozen in liquid nitrogen, and stored at −80°C until analysis.

2.2 Reagents and Chemicals

Dibenzo[*def,p*]chrysene was purchased from Midwest Research Institute (Kansas City, MO). Unlabeled (±)-*anti*-*cis*-DBCDE-dA and (±)-*anti*-*trans*-DBCDE-dA standards, and ^{15}N-labeled (±)-*anti*-*cis*-DBCDE-dA and (±)-*anti*-*trans*-DBCDE-dA standards were synthesized by the laboratory of Dr. Shantu Amin at Penn State University.

2.3 Preparation of DNA

DNA was isolated from frozen tissue using Qiagen Genomic Tip 500/G (Qiagen, Germantown, MD) or Roche DNA Isolation Kit for Cells and Tissues (Roche, Indianapolis, IN) as described by the manufacturer. One hundred μg of DNA in a final volume of 450 μl water with 10 mM $MgCl_2$ was submitted to a series of enzymatic steps to prepare individual deoxynucleotides: 1) 375 units Dnase I (Life Technologies, Carlsbad, CA) at 37°C for 1.5 hours; 2) 7 units nuclease P1 (Sigma-Alrich, St. Louis, MO) at 37°C for 1.5 hours; 3) 30 units shrimp alkaline phosphatase (Thermo Scientific, Waltham, MA) at 37°C for 1 hours. After DNA digestion, a 50 μl aliquot was set aside for HPLC base analysis. Forty pg of ^{15}N-labeled (±)-*anti*-*cis*-DBCDE-dA and (±)-*anti*-*trans*-DBCDE-dA was spiked into each sample to serve as an internal standard. One ml ethanol was added to each sample and the sample was incubated at −20°C overnight. The following day the samples were centrifuged at 14,000g for 10 minutes at 4°C. The supernatant was then transferred to a new 1.7 ml microcentrifuge tube and evaporated under a nitrogen stream to concentrate the sample to 50 μl. Fifty μl of methanol was added to bring the samples to 100 μl (1 μg DNA/μl). The samples were filtered through a costar-X spin tube before being transferred to an autosampler vial.

2.4 HPLC Base Analysis

The aliquot of digested DNA reserved from sample preparation for adduct analysis was subjected to HPLC analysis using an Alliance 2695 HPLC (Waters, Milford, MA) with a 2996 photodiode array detector (PDA), and a Luna 3 μm C_{18}, 150 × 3 mm column (Phenomenex, Torrance, CA). Solvent A was 20 mM ammonium formate (pH 4.5), and solvent B was acetonitrile. The flow rate was 0.4 ml per minute. The gradient used was 99% A and 1% B for 3 minutes, followed by a 12 minute ramp from 99% A to 60% A and 1% B to 40% B. The column and samples were kept at 30°C during the run. A wavelength of 254

ηm was chosen for sample detection. Deoxyguanosine (dG) and deoxyadenosine (dA) standards eluted at 9.3 and 10.2 minutes respectively. A calibration curve for each standard was constructed and sample base levels were calculated by interpolation of the curve using Empower 2 software (Waters, Milford, MA). The number of dA calculated in each sample was used to present the data as DBCDE-dA/1×10^8 dA.

2.5 Stable isotope dilution UHPLC-MS/MS

Adduct analysis was performed using a 4000 QTRAP hybrid triple quadrupole/linear ion trap LC-MS/MS system (AB Sciex, Redwood City, CA) interfaced with a Flexar UHPLC system (Perkin-Elmer, Waltham, MA) using an Acuity UPLC 1.7 μm BEH C_{18}, 100 × 2.1 mm column (Waters, Milford, MA). The UHPLC solvent method utilized a gradient of solvent A (5 mM NH_4OAc + 0.1% formic acid in HPLC grade water) and solvent B (acetonitrile) at a flow rate of 500 μl/min. The 7.5 minute gradient was as follows: 1) 0.5 minute 80% A and 20% B; 2) 6 minutes to 10% A and 90% B; 3) 0.1 min 10% A and 90% B; 4) 0.9 minute wash out 10% A and 90% B. The MS parameters were set as follows: electrospray ionization – positive mode; electrospray source temperature – 600°C; declustering potential – 60 eV; collision energy – 30 eV; entrance potential – 10 eV; cell exit potential – 10 eV; collision activated dissociation gas – high; curtain gas – 20 psi. Adducts were analyzed in multiple reaction monitoring (MRM) mode with the following transitions 604.2/335.0, 604.2/317.0, 604.2/289.1 (targeted adducts) and 609.2/335.0, 609.2/317.0, 609.2/289.1 (internal standards). Peak integration was performed using Analyst 1.5.2 Software (AB Sciex, Redwood City, CA).

2.5.1 Method Validation—The UHPLC-MS/MS method was validated by spiking 100 μg of control sample matrix with fixed amounts of (±)-*anti*-*cis*-DBCDE-dA internal standard and increasing amounts of unlabeled (±)-*anti*-*cis*-DBCDE-dA (0.05, 0.12, 0.17, 0.50, 1.66 fmol/μl) and plotting the observed concentrations against the spiked concentrations.

2.5.2 Calibration Curve—A calibration curve for each adduct isomer was set up using unlabeled (±)-*anti*-*cis*-DBCDE-dA and (±)-*anti*-*trans*-DBCDE-dA adducts (0.1, 0.3, 3.0 pg/μl) mixed with 0.4 pg/μl ^{15}N-labeled adducts in a 100 μg DNA matrix.

2.6 Statistical Analysis

Statistical analysis was carried out using Prism 6.0 (Graphpad, La Jolla, CA). One-way Analysis of Variance (Anova) with Tukey's multiple comparisons test was carried out to determine significant difference in adduct formation between tissues in treatments groups and isomers within the same treatment. A p-value of ≤ 0.05 was considered significant. Percentage of adducts was calculated using the following equation: (Total Adducts WT) – (Total Adducts KO)/(Total Adducts WT).

3. Results

3.1 UHPLC-MS/MS Method Validation

The UHPLC-MS/MS method was validated using a spiked control matrix (0.05, 0.12, 0.17, 0.50, 1.66 fmol/μl) and plotting the measured analyte concentrations against the spiked

concentrations. Linear regression revealed an R^2 of 0.999 with a slope of 0.997 indicating accurate quantitation with the developed protocol (Figure 2). The limit of quantitation (LOQ) was determined to be 0.12 fmol/μg DNA (10 times signal-to-noise ratio) using standards prepared as described in Materials and Methods 2.5.1.

Although the (−)-*anti-cis* and (−)-*anti-trans* isomers are the major stereoisomers formed after CYP 1B1 metabolism in mammalian systems, our 7.5 minute UHPLC-MS/MS method did not separate the ^{15}N-labeled optically distinct (−)-*anti-cis* from the (+)-*anti-cis*, nor the (−)-*anti-trans* from the (+)-*anti-trans* internal standards. As a result we are not able to definitively distinguish the (−) and (+) stereoisomers, but are confident the overwhelming majority of the adducts are (−)-*anti* isomers based on previous studies characterizing DBC bioactivation and adduction [6, 17, 18].

3.2 Identification and Quantitation of DBCDE-dA adducts after oral exposure

Successful identification of the target (±)-*anti-cis*-DBCDE-dA and (±)-*anti-trans*-DBCDE-dA adduct isomers with co-elution of spiked internal standards is indicated by the two peaks in the representative MRM chromatogram using liver DNA from a WT gavaged mouse (Figure 3). Calibration curves for both isomers appear to be linear (Figure 3 inset).

Figure 4A represents adduct formation in the spleen of WT and *Cyp1b1* KO mice. Statistical analysis indicates the formation of (±)-*anti-cis*-DBCDE-dA and (±)-*anti-trans*-DBCDE-dA adducts are significantly decreased in the spleen of *Cyp1b1* KO mice compared to gavaged WT mice (Figure 4A). Additionally, the (±)-*anti-trans* adduct is formed preferentially over the (±)-*anti-cis* adduct in the gavaged WT group. Adduct levels in the thymus of WT and *Cyp1b1* KO mice were below the LOQ, making meaningful interpretation unreliable.

Furthermore, we measured adduct formation in the liver and lung for both treatment groups (Figure 4B and 4C). In gavaged WT mice the (±)-*anti-trans* adduct is formed at significantly higher levels than the (±)-*anti-cis* adduct in both organs consistent with adduct formation in the spleen. *Cyp1b1* KO adducts in the liver and lung are significantly reduced in each tissue as expected based on predominant DBCDE formation by Cyp1b1 [9, 20]. The (±)-*anti-trans* isomer is preferentially formed in *Cyp1b1* KO liver, whereas the (±)-*anti-cis* and (±)-*anti-trans* isomers in *Cyp1b1* KO lung are formed at comparable levels.

4. Discussion

The primary mechanism for DBC induced carcinogenesis occurs through the formation of covalently bound DBCDE-DNA adducts resulting in genotoxicity [21]. Additionally, PAH genotoxicity is correlated with immunotoxicity [14]. This study provides the first evidence of DBC-adduct formation in the spleen of mice treated orally with DBC (Figure 4). Adduct identification provides mechanistic support for the immunosuppressive properties of DBC established previously using T-cell dependent and independent antibody response assays [15, 16]. Using a UHPLC-MS/MS method we are able to quantitate (±)-*anti-cis*-DBCDE-dA (45 DBCDE-dA/1×10^8 dA) and (±)-*anti-trans*-DBCDE-dA (58 DBCDE-dA/1×10^8 dA) adducts in the spleen of WT mice euthanized 3 days after 5 consecutive days of oral gavage with 10 mg/kg DBC. Identification of the (±)-*anti-cis* and (±)-*anti-trans* adducts is

consistent with the stereoselectivity reported in other DBC target tissues (Figure 3) [6, 7, 11, 18]. Direct application of DBC to the oral cavity by Zhang et al. [18] resulted in high levels of adduct formation surpassing the current study's maximum measured level (116 (±)-*anti-trans*-DBCDE-dA/1×10^8 dA). However, our route of administration (oral gavage) differs significantly compared to direct application of the target tissue making direct comparison of the two studies difficult.

In the current study DBCDE-dA adducts detected in the thymus were below the LOQ for the method. Lauer et al. [15], reported DBC exposure results in a greater T-cell-dependent antibody response than a T-cell-independent antibody response suggesting low level adduct formation in the thymus may contribute to the T-cell dependent-immunosuppression identified in the spleen. However, we do not know the level of adduct formation required for DBC-mediated immunosuppression emphasizing the need for future studies investigating DBC genotoxicity and immunosuppression. Furthermore, we provide the first evidence using a highly sensitive UHPLC-MS/MS method that the loss of Cyp1b1 expression significantly reduces adduct formation in the spleen, lung, and liver (Figure 4). Reduced adduct formation in *Cyp1b1* KO mice support earlier studies identifying Cyp1b1 as the major Cyp responsible for DBCDE-dA adduct formation [5, 9, 11]. Cyp1b1 is also critical for DMBA-induced spleen cell immunotoxicity in mice [22]. The spleen is known for high levels of constitutive Cyp1b1 expression, and as a result is susceptible to genotoxicity through bioactivation [14, 23]. The reduced adduct formation identified in the spleen would suggest *Cyp1b1* KO mice should be less susceptible to DBC-mediated splenic immunotoxicity.

DBC adduct formation in the liver of *Cyp1b1* KO mice retained the *cis:trans* (2:5) ratio identified in the liver of the gavaged WT group, whereas lung and spleen isomer formation occurred at equal levels. Adduct formation in the lung of *Cyp1b1* KO animals is lower than expected based on a previous study using *Cyp1b1* KO mice reporting oral treatment with DBC reduces tumor incidence and restricts carcinogenic lesions to the lung [5]. Although adduct formation was not examined, the high number of lung lesions found by Buters et al. [5], were attributed to Cyp1a1 bioactivation and DBCDE-adduct genotoxicity. Supporting studies performed using V79 Chinese hamster cells stably expressing either human, rat, or mouse CYP1A1 or CYP1B1 indicate only mouse Cyp1a1 is able to form the nonpolar DBCDE-adducts associated with Cyp1b1 bioactivation [5, 20]. Using *Cyp1b1* KO mice, the current study reports additional mouse Cyp enzymes (most likely 1a1) are capable of forming DBCDE-adducts, but at low levels suggesting other factors may be contributing substantially to DBC carcinogenicity in the lung. Further investigation is necessary to fully understand CYP1B1 and 1A1 mechanism(s) of carcinogenicity and immunotoxicity.

5. Conclusion

Using a highly sensitive UHPLC-MS/MS method we identified for the first time DBCDE-dA adduct formation in the spleen of mice providing linkage between DBC exposure and immunotoxicity. Furthermore, utilizing *Cyp1b1* KO mice we show Cyp1b1 is responsible for 71% of DBCDE-dA adducts formed in the spleen. Taking Cyp1b1 bioactivation into account the current study suggests *Cyp1b1* KO mice should be less susceptible to DBC-

induced immunotoxicity. The high levels of DBC-DNA adducts identified in the spleen, along with the known high levels of Cyp1b1 expression in this organ, supports further investigation into DBC-mediated immunotoxicity.

Acknowledgements

The authors would like to thank Dr. Frank Gonzalez of the National Cancer Institute for providing the *Cyp1b1* KO mice and Dr. Shantu Amin for providing the DBCDE-dA standards. Additionally, the authors would like to thank Beth Siddens for her help with the DNA digestion protocol, and Erin Madeen for her help with the HPLC base analysis protocol. This study was supported by the NIH grants P42 ES016465, P30 ES000210, R01 ES019968 and P01CA90890. TAH was supported by T32 ES007060.

Abbreviations

DBC	dibenzo[*def,p*]chrysene
DBCDE	dibenozo[*def,p*]chrysene-(±)-11,12-dihydrodiol-13,14-epoxide
PAH	polycyclic aromatic hydrocarbon
BaP	benzo[*a*]pyrene
DMBA	7,12,-dimethylbenz[*a*]anthracene
EPHX1	epoxide hydrolase
TDAR	T cell-dependent antibody response
UHPLC	ultra-high performance liquid chromatography
MS/MS	tandem mass spectrometry
MRM	multiple reaction monitoring
LOQ	limit of quantitation
CYP	cytochrome P450
dA	deoxyadenosine

References

1. Jia Y, Stone D, Wang W, Schrlau J, Tao S, Simonich SL. Estimated reduction in cancer risk due to PAH exposures if source control measures during the 2008 Beijing Olympics were sustained. Environmental Health Perspectives. 2011; 119:815–820. [PubMed: 21632310]
2. Mumford JL, Li X, Hu F, Lu XB, Chuang JC. Human exposure and dosimetry of polycyclic aromatic hydrocarbons in urine from Xuan Wei, China with high lung cancer mortality associated with exposure to unvented coal smoke. Carcinogenesis. 1995; 16:3031–3036. [PubMed: 8603481]
3. Orris L, Van Duuren BL, Kosak AI, Nelson N, Schmitt FL. The carcinogenicity for mouse skin and the aromatic hydrocarbon content of cigarette-smoke condensates. Journal of the National Cancer Institute. 1958; 21:557–561. [PubMed: 13576107]
4. IARC. Some non-heterocyclic polycyclic aromatic hydrocarbons and some realted exposures. IARC monographs on the evaluation of carcinogenic risks to humans / World Health Organization, International Agency for Research on Cancer. 2010; 92:1–853.
5. Buters JT, Mahadevan B, Quintanilla-Martinez L, Gonzalez FJ, Greim H, Baird WM, Luch A. Cytochrome P450 1B1 determines susceptibility to dibenzo[a,l]pyrene-induced tumor formation. Chemical Research in Toxicology. 2002; 15:1127–1135. [PubMed: 12230405]

6. Chen KM, Zhang SM, Aliaga C, Sun YW, Cooper T, Gowdahalli K, Zhu J, Amin S, El-Bayoumy K. Induction of ovarian cancer and DNA adducts by Dibenzo[a,l]pyrene in the mouse. Chemical Research in Toxicology. 2012; 25:374–380. [PubMed: 22107356]
7. Ralston SL, Lau HH, Seidel A, Luch A, Platt KL, Baird WM. The potent carcinogen dibenzo[a,l]pyrene is metabolically activated to fjord-region 11,12-diol 13,14-epoxides in human mammary carcinoma MCF-7 cell cultures. Cancer Research. 1994; 54:887–890. [PubMed: 8313376]
8. Arif JM, Gupta RC. Microsome-mediated bioactivation of dibenzo[a,l]pyrene and identification of DNA adducts by 32P-postlabeling. Carcinogenesis. 1997; 18:1999–2007. [PubMed: 9364012]
9. Luch A, Coffing SL, Tang YM, Schneider A, Soballa V, Greim H, Jefcoate CR, Seidel A, Greenlee WF, Baird WM, Doehmer J. Stable expression of human cytochrome P450 1B1 in V79 Chinese hamster cells and metabolically catalyzed DNA adduct formation of dibenzo[a,l]pyrene. Chemical Research in Toxicology. 1998; 11:686–695. [PubMed: 9625737]
10. Luch A, Kishiyama S, Seidel A, Doehmer J, Greim H, Baird WM. The K-region trans-8,9-diol does not significantly contribute as an intermediate in the metabolic activation of dibenzo[a,l]pyrene to DNA-binding metabolites by human cytochrome P450 1A1 or 1B1. Cancer Research. 1999; 59:4603–4609. [PubMed: 10493514]
11. Ralston SL, Seidel A, Luch A, Platt KL, Baird WM. Stereoselective activation of dibenzo[a,l]pyrene to (−)-anti (11R,12S,13S,14R)- and (+)-syn(11S,12R,13S,14R)-11,12-diol-13,14-epoxides which bind extensively to deoxyadenosine residues of DNA in the human mammary carcinoma cell line MCF-7. Carcinogenesis. 1995; 16:2899–2907. [PubMed: 8603462]
12. Kropachev K, Kolbanovskiy M, Liu Z, Cai Y, Zhang L, Schwaid AG, Kolbanovskiy A, Ding S, Amin S, Broyde S, Geacintov NE. Adenine-DNA adducts derived from the highly tumorigenic Dibenzo[a,l]pyrene are resistant to nucleotide excision repair while guanine adducts are not. Chemical Research in Toxicology. 2013; 26:783–793. [PubMed: 23570232]
13. Page TJ, O'Brien S, Holston K, MacWilliams PS, Jefcoate CR, Czuprynski CJ. 7,12-Dimethylbenz[a]anthracene-induced bone marrow toxicity is p53-dependent. Toxicological Sciences. 2003; 74:85–92. [PubMed: 12730609]
14. Uno S, Dalton TP, Dragin N, Curran CP, Derkenne S, Miller ML, Shertzer HG, Gonzalez FJ, Nebert DW. Oral benzo[a]pyrene in Cyp1 knockout mouse lines: CYP1A1 important in detoxication, CYP1B1 metabolism required for immune damage independent of total-body burden and clearance rate. Molecular Pharmacology. 2006; 69:1103–1114. [PubMed: 16377763]
15. Lauer FT, Walker MK, Burchiel SW. Dibenzo[def,p]chrysene (DBC) suppresses antibody formation in spleen cells following oral exposures of mice. Journal of Toxicology and Environmental Health. Part A. 2013; 76:16–24. [PubMed: 23151208]
16. Li Q, Lauer FT, Liu KJ, Hudson LG, Burchiel SW. Low-dose synergistic immunosuppression of T-dependent antibody responses by polycyclic aromatic hydrocarbons and arsenic in C57BL/6J murine spleen cells. Toxicology and Applied Pharmacology. 2010; 245:344–351. [PubMed: 20353797]
17. Luch A. On the impact of the molecule structure in chemical carcinogenesis. Exs. 2009; 99:151–179. [PubMed: 19157061]
18. Zhang SM, Chen KM, Aliaga C, Sun YW, Lin JM, Sharma AK, Amin S, El-Bayoumy K. Identification and quantification of DNA adducts in the oral tissues of mice treated with the environmental carcinogen dibenzo[a,l]pyrene by HPLC-MS/MS. Chemical Research in Toxicology. 2011; 24:1297–1303. [PubMed: 21736370]
19. Mahadevan B, Luch A, Bravo CF, Atkin J, Steppan LB, Pereira C, Kerkvliet NI, Baird WM. Dibenzo[a,l]pyrene induced DNA adduct formation in lung tissue in vivo. Cancer Letters. 2005; 227:25–32. [PubMed: 16051029]
20. Luch A, Schober W, Soballa VJ, Raab G, Greim H, Jacob J, Doehmer J, Seidel A. Metabolic activation of dibenzo[a,l]pyrene by human cytochrome P450 1A1 and P450 1B1 expressed in V79 Chinese hamster cells. Chemical Research in Toxicology. 1999; 12:353–364. [PubMed: 10207125]
21. Melendez-Colon VJ, Luch A, Seidel A, Baird WM. Cancer initiation by polycyclic aromatic hydrocarbons results from formation of stable DNA adducts rather than apurinic sites. Carcinogenesis. 1999; 20:1885–1891. [PubMed: 10506100]

22. Gao J, Lauer FT, Dunaway S, Burchiel SW. Cytochrome P450 1B1 is required for 7,12-dimethylbenz(a)-anthracene (DMBA) induced spleen cell immunotoxicity. Toxicological Sciences. 2005; 86:68–74. [PubMed: 15843505]

23. Bieche I, Narjoz C, Asselah T, Vacher S, Marcellin P, Lidereau R, Beaune P, de Waziers I. Reverse transcriptase-PCR quantification of mRNA levels from cytochrome (CYP)1, CYP2 and CYP3 families in 22 different human tissues. Pharmacogenetics and Genomics. 2007; 17:731–742. [PubMed: 17700362]

Highlights

- Stable-isotope dilution UHPLC-MS/MS was used to detect DBCDE-dA adducts
- DBCDE-dA adducts were identified at high levels in the spleen of wild-type mice
- *Cyp1b1* KO mice have significantly reduced adducts in liver, lung, and spleen
- Cyp1b1 accounts for 71% of DBCDE-dA adducts formed in the spleen

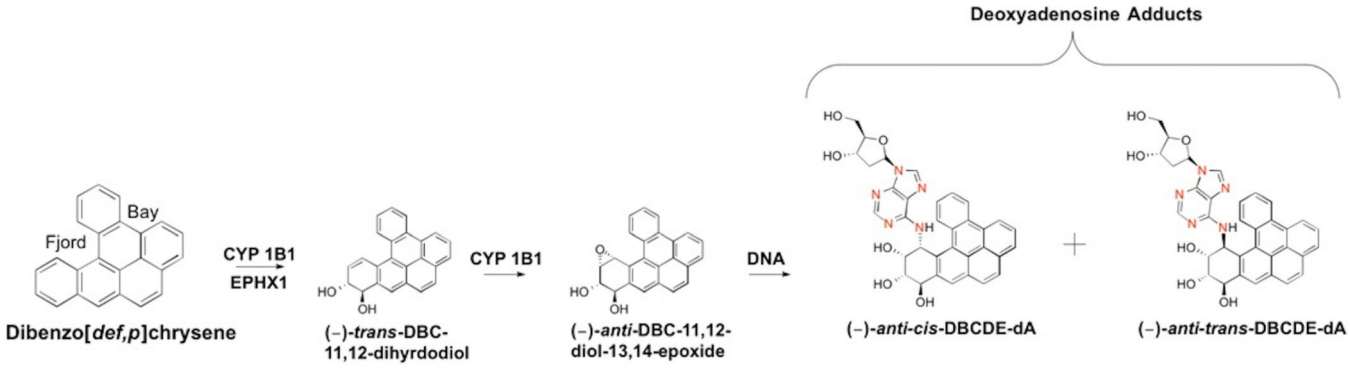

Figure 1. Schematic of DBC bioactivation to DBC-11,12-diol-13,14-epoxide (DBCDE) by cytochrome P450 1B1 and EPHX1

In the presence of DNA DBCDE binds covalently to DNA preferentially at the N^6-position of deoxyadenosine forming the major adducts (−)-*anti-cis*-DBCDE-dA and (−)-*anti-trans*-DBCDE-dA. Location of stable ^{15}N isotopes incorporated into the internal standards are shown in red.

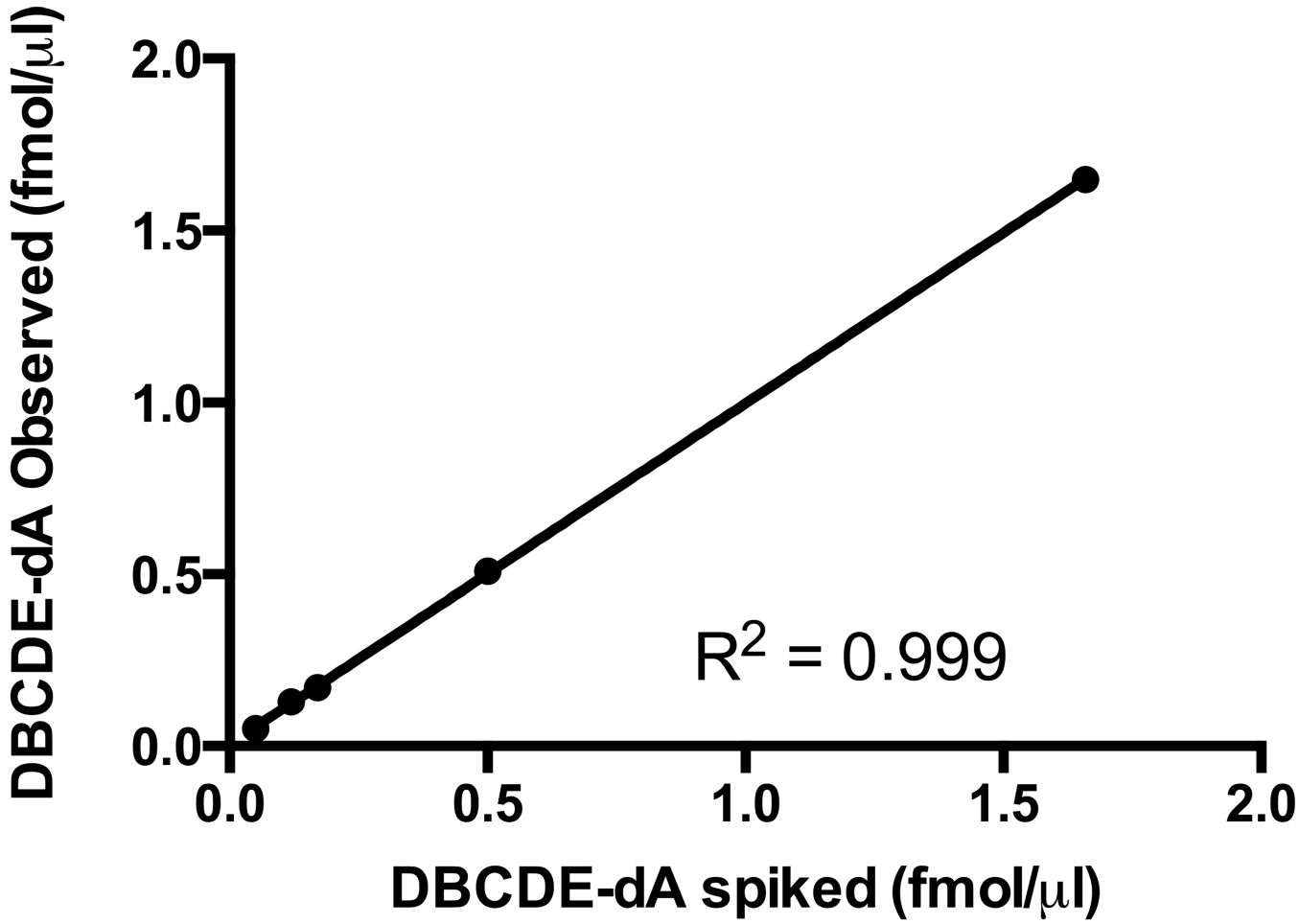

Figure 2. UHPLC-MS/MS method validation

The stable-isotope dilution UHPLC-MS/MS method was validated using 100 μg spiked control matrix (0.05, 0.12, 0.17, 0.50, 1.66 fmol/μl (±)-*anti*-*cis*-DBCDE-dA) and plotting the measured analyte concentrations against the spiked concentrations. Linear regression revealed an R^2 of 0.999 with a slope of 0.997 indicating accurate quantitation with the developed protocol. The limit of quantitation (LOQ) was determined to be 0.12 fmol/μg DNA (10 times signal-to-noise ratio).

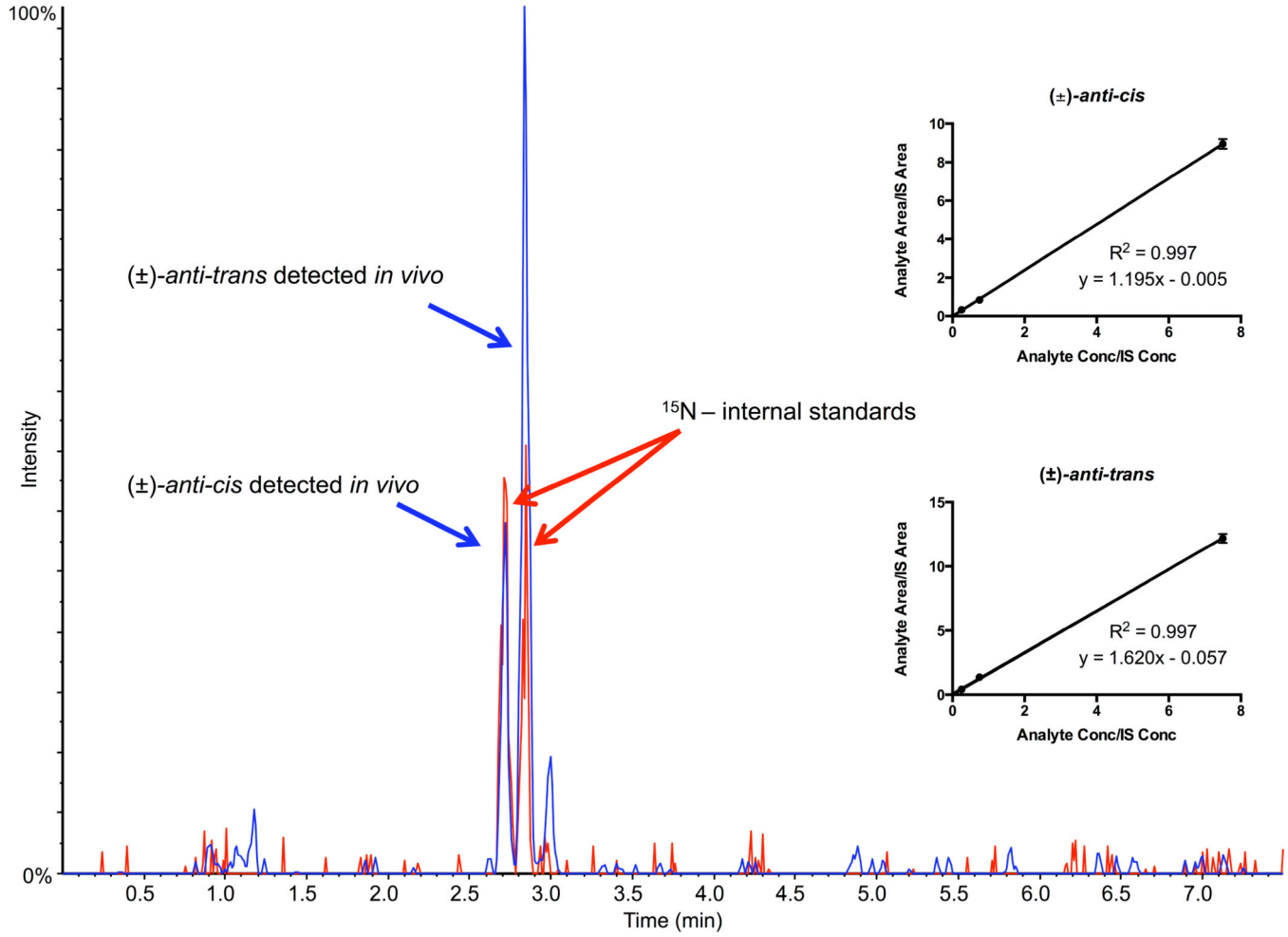

Figure 3. Representative MRM chromatogram of (±)-*anti*-DBCDE-dA adducts obtained from mice orally exposed to 10 mg/kg DBC for 5 days and euthanized 3 days after final exposure

The chromatogram shows separation of major adducts (±)-*anti-cis*-DBCDE-dA and (±)-*anti-trans*-DBCDE-dA using the 7.5-minute stable-isotope dilution UPLC-MS/MS method. The blue peaks represent the target adducts (*m/z* 604.2 → *m/z* 335.0) detected *in vivo*, while the red peaks represent the spiked ^{15}N-labeled (±)-*anti-cis*-DBCDE-dA and (±)-*anti-trans*-DBCDE-dA internal standards (*m/z* 609.2 → *m/z* 335.0). Figure insets represent linear calibration curves for each (±)-*anti-cis*-DBCDE-dA and (±)-*anti-trans*-DBCDE-dA adduct.

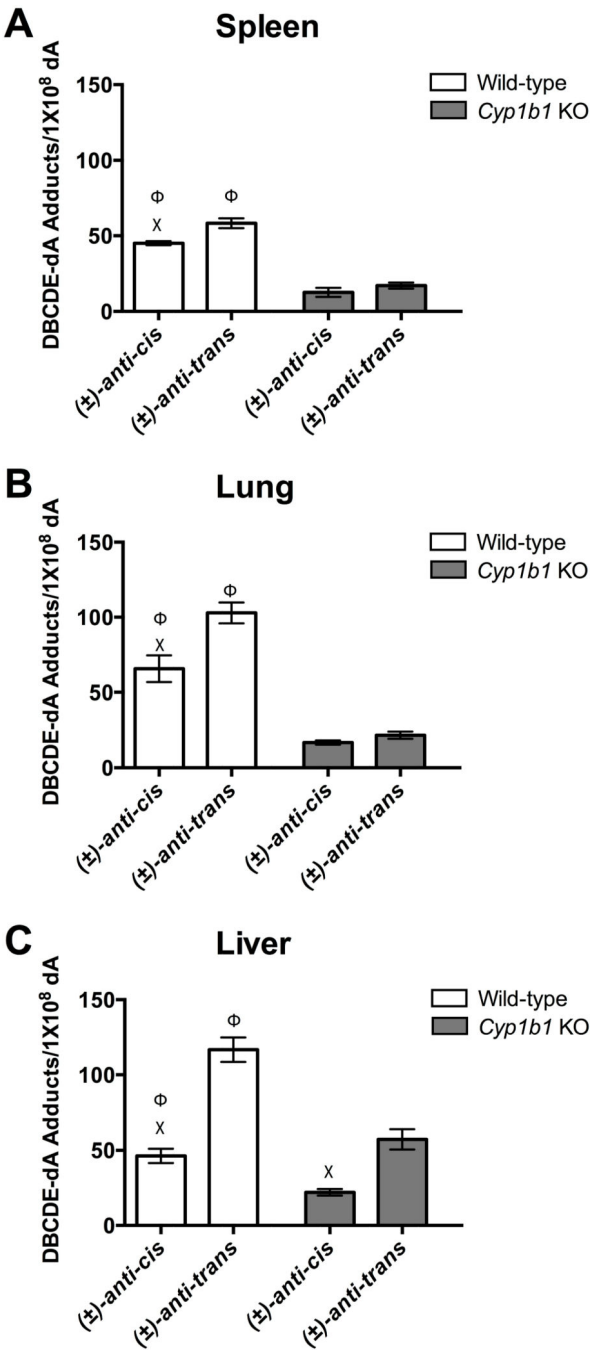

Figure 4. DBCDE-dA Adduct Quantitation

Quantitation of (±)-*anti-cis*-DBCDE-dA and (±)-*anti-trans*-DBCDE-dA adducts in spleen (A), lung (B), and liver (C) of wild-type (n = 4) or *Cyp1b1* KO (n = 5) mice exposed orally to 10 mg/kg DBC daily for 5 days and euthanized 3 days after the final exposure. All tissue from WT mice gavaged (white bars) had significantly higher levels of (±)-*anti-trans*-DBCDE-dA adduct formation compared to (±)-*anti-cis*-DBCDE-dA adducts consistent with previous studies. Additionally, the loss of Cyp1b1 (light grey bars) significantly reduced both adducts in all three tissues. One-way Analysis of Variance (Anova) with Tukey's

multiple comparisons test was carried out to determine significant difference in adduct formation between tissues within different treatment groups and isomers within the same treatment. A p-value of ≤ 0.05 was considered significant. (X = significant difference between (±)-*anti-cis*-DBCDE-dA and (±)-*anti-trans*-DBCDE-dA adducts of the same tissue and treatment group; Φ = significant difference between indicated isomer for treatment and *Cyp1b1* KO group